IEEE Access
Multidisciplinary ⋮ Rapid Review ⋮ Open Access Journal

Received 14 March 2023, accepted 18 April 2023, date of publication 26 April 2023, date of current version 3 May 2023.

Digital Object Identifier 10.1109/ACCESS.2023.3270773

RESEARCH ARTICLE

Data Driven Model Predictive Control for Modular Multilevel Converters With Reduced Computational Complexity

MUNEEB MASOOD RAJA, HAORAN WANG, MUHAMMAD HASEEB ARSHAD, GREGORY J. KISH, (Senior Member, IEEE), AND QING ZHAO, (Member, IEEE)
Department of Electrical and Computer Engineering, University of Alberta, Edmonton, AB T6G 2R3, Canada
Corresponding author: Qing Zhao (qingz@ualberta.ca)

ABSTRACT Model predictive control (MPC) has become increasingly popular among researchers for modular multilevel converters (MMCs) due to its ability to incorporate multiobjective control and provide superior dynamic response. However, it is computationally challenging to implement it on MMCs when the number of submodules is increased. This paper proposes a finite control set (FCS) model predictive control (MPC) with reduced computational complexity for modular multilevel converters (MMCs). To accomplish this goal, a reduced order data-driven model is obtained using sparse identification of nonlinear systems (SINDy) by incorporating the input terms in the load current and circulating current dynamics. As a result, the need to use the arm voltages or the submodule capacitor voltages dynamic equations as in the case of a conventional FCS-MPC is eliminated. To improve the output current total harmonic distortion (THD) and reduce the effect of higher switching frequencies caused by the FCS-MPC, an updated cost function is proposed. The effectiveness of the proposed technique is validated by simulation and experimental results.

INDEX TERMS FCS-MPC, MMCs, data-driven control, SINDy, power converters.

I. INTRODUCTION

Over the past decade, modular multilevel converters (MMCs) have gathered immense attention in high/medium voltage applications due to their modularity, scalability, and low switching losses. The applications of MMCs include but are not limited to HVDC power transmission [1], motor drives [2], energy storage system [3], and power electronic transformers [4]. Due to the wide range of applications, developing efficient control strategies for MMCs is important.

The conventional cascaded linear control structure developed for MMCs has limitations in terms of the performance of the dynamic response [5]. Also, the control complexity increases due to the addition of more control loops when circulating current and voltage balancing are also included in the control [6], [7], [8]. On the other hand, pulse width modulation (PWM) constitutes a part of the control and removal of the modulation step from the converter control can simplify the control design and implementation [9].

A finite control set model predictive control (FCS-MPC) is an optimal control that provides better transient response without the intervention of the intermediate modulation step [10]. Additionally, it predicts the plant's future behavior by using the explicit plant model and can handle multiobjective optimization and nonlinear constraints problems. The FCS-MPC can generate the optimal combination of switching states that minimizes a given cost function and can provide the control signals directly to the converter [11]. A comparative study between classical and MPC control implemented on MMCs is conducted by [12] and [13] in which the MPC produced better circulating current control and a superior dynamic response while requiring fewer control parameters to tune.

In spite of some remarkable features of the FCS-MPC, there are challenges faced by researchers in implementing this control strategy. As the MPC relies heavily on the model, uncertainties in the physical system cause inevitable errors

The associate editor coordinating the review of this manuscript and approving it for publication was Ki-Bum Park.

and online identification techniques [14] may be required to improve the robustness. Secondly, FCS-MPC produces high switching frequencies which reduces system efficiency. The high switching frequency also increases unnecessary switching which may cause reliability issues [15], [16]. Finally, one of the major challenges in implementing the MPC is the added computational complexity when the number of submodules (SMs) is increased.

Many efforts have been made to deal with these problems. In [17], the authors proposed a nonlinear MPC algorithm for MMC-HVDC with a reduced number of active voltage vectors to alleviate the computational load and the switching losses. A direct FCS-MPC was proposed in [13] which computes 2^{2N} control options at each time step as opposed to C_N^{2N} control sets shown in [18]. Even though the direct FCS-MPC approach is relatively easy to implement, it becomes impractical to implement it on a large-scale MMC system due to the exponential increase in the number of control options as the number of SMs grows. An indirect FCS-MPC technique was proposed by [19] in which the capacitor voltage balancing was decoupled from the MPC formulation and performed in a separate block to bring the number of control options down to only $(N+1)^2$ while maintaining $2N+1$ output voltage levels. Several studies [17], [20], [21] have been performed that use $N+1$ voltage levels configuration to further reduce the computational complexity. Nevertheless, the output current THD performance is degraded as compared to the $2N+1$ voltage levels configuration. This issue was later addressed in [22] by using a preselection algorithm to evaluate the control options. Recently, a machine learning emulation of MPC for MMCs has been developed in [23] to reduce the computational burden of MPC. Therein, the authors implemented an emulation of MPC by training a neural network model using the data acquired through a standard FCS-MPC.

To deal with the high frequency issue, [17] presented a finite-level-set MPC to account for output current, circulating current, switching frequency, and SM capacitor voltage using a reduced number of switching states. Later, FCS-MPC with optimized pulse patterns was developed by [24] and [25] to decrease the switching frequency. This allows superior harmonic performance under low switching frequency operation. Recently, [11] investigated the use of event-triggered neural-predictor-based FCS-MPC for low switching frequency operation, allowing the controller to deal with uncertainties and unnecessary energy loss.

Many techniques have been developed in the literature to obtain data-driven models. Some of them include autoregressive models [26], [27], and neural network (NN) and deep reinforcement learning models [28], [29], [30]. Neural network based models are widely adopted due to the rapid increase in the available processing power. However, these models lack interpretability and require a large amount of data for training. Overfitting is also a cause of concern for NN based models. Similarly, in the event of abrupt changes in the system, the controller must be able to act quickly to compensate for the changes introduced in the system dynamics, allowing a short span of time for model discovery. The recently developed SINDy framework [31] allows the use of limited data while relying on sparsity-promoting optimization to identify parsimonious systems. This results in producing interpretable models that avoid overfitting.

This paper presents a novel and effective data-driven technique to implement a FCS-MPS on MMCs to tackle two of the major problems that occur while implementing a conventional FCS-MPC without complicating the control design. The control algorithm is designed to reduce the computational complexity and improve the output current THD performance along with reducing the high switching frequency. The computational complexity is reduced by developing a reduced state data-driven model for the MMC using sparse identification of nonlinear systems (SINDy). When applying SINDy, the model is trained by including the input switching terms in the dynamic equations for circulating current and output current, thereby eliminating the need to evaluate the corresponding SM capacitor voltages or the arm voltages, which are usually obtained from some mathematical models commonly used in the existing literature for computing the cost function of the FCS-MPC. To further reduce the computational complexity, the capacitor voltage balancing is decoupled from the control, and a separate voltage balancing block is implemented. Furthermore, the trained model provides better estimates of system states as compared to the conventional average models used in the literature, hence increasing the accuracy of the MPC prediction. Finally, in the proposed FCS-MPC, the cost function is modified by adding a weighing factor to the switching terms to ensure better THD performance for the output current while reducing the high switching frequency effect caused by FCS-MPC. The effectiveness of the proposed technique is verified using simulation and experimental results and it is shown that the proposed data-driven MPC strategy offers a novel and efficient solution to controlling MMCs.

The rest of the paper is organized as follows. Section II describes the MMC topology and mathematical models used in the literature. In Section III, the proposed SINDy model is described. The proposed FCS-MPC formulation is discussed in Section IV. In Sections V and VI, simulation and experimental results are presented to validate the proposed scheme. Finally, the conclusion is made in Section VII.

II. SYSTEM MODELING OF MMC

A. MMC TOPOLOGY

Fig. 1 shows the three-phase MMC with each leg having a upper and a lower arm. The two arms are connected through an arm inductance L. Each arm consists of N cascaded SMs. A half bridge topology is considered in this research as it is the most commonly used topology. Each SM is constructed using a capacitor connected to two in-series switches. The upper and lower arm currents in three phases are denoted by i_{ua}, i_{la}, i_{ub}, i_{lb}, i_{uc}, and i_{lc}, respectively. The subscript u, l

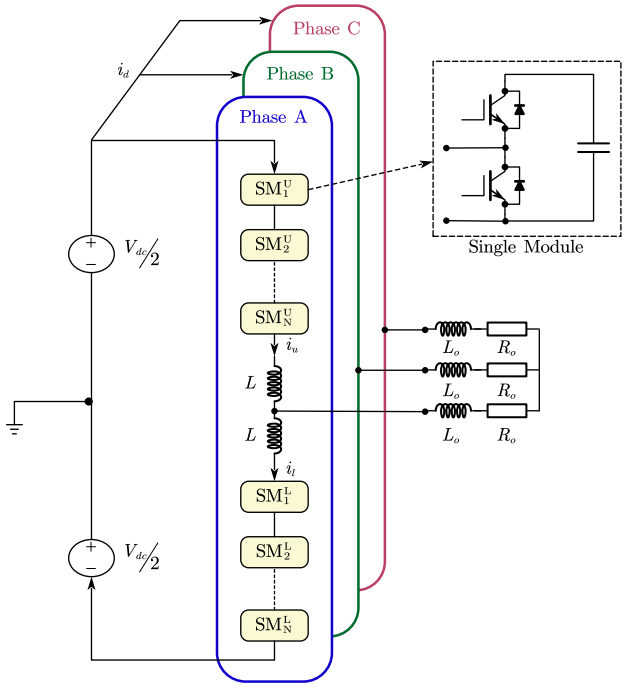

FIGURE 1. Modular multilevel converter schematic diagram.

represents upper and lower arms, and $a, b,$ and c denotes the corresponding phase, respectively. For simplicity, all the relationships will be represented for a single phase MMC as they are identical and the subscripts for the phases are dropped.

B. MATHEMATICAL MODELING

In the literature, there are two different mathematical models that are widely used while implementing FCS-MPC. The main difference lies in the definition of states, in which the sum of capacitor voltages in upper and lower arms are taken as states in one of them, whereas individual SM capacitor voltages are taken as states in the other. Both mathematical models are derived using the Kirchhoff's current and voltage laws.

The first model is given by the following dynamic equations:

$$\begin{cases} \dfrac{di_o}{dt} = \dfrac{1}{2L_o + L}(v_l - v_u - 2Ri_o) \\ \dfrac{di_c}{dt} = \dfrac{1}{2L}(V_{dc} - v_l - v_u) \\ \dfrac{dv_{\Sigma u}}{dt} = \dfrac{n_u}{C} i_u \\ \dfrac{dv_{\Sigma l}}{dt} = \dfrac{n_l}{C} i_l \end{cases} \tag{1}$$

where C is the submodule capacitance, i_o is the output current, i_c is the circulating current, $v_{\Sigma u}$ is the sum of capacitor voltages in the upper arm, $v_{\Sigma l}$ is the sum of capacitor voltages in the lower arm, and n_u and n_l are the number of active switches in the upper and lower arms, respectively. The upper arm voltage v_u and lower arm voltage v_l is computed based on the assumption that all the capacitor voltages are well balanced and is given below:

$$v_u = \frac{n_u}{N} v_{\Sigma u} \tag{2}$$

$$v_l = \frac{n_l}{N} v_{\Sigma l} \tag{3}$$

The relationship between the upper and lower arm currents with the output and circulating currents is as under:

$$i_o = i_u - i_l \tag{4}$$

$$i_c = \frac{1}{2}(i_u + i_l) \tag{5}$$

The second model on the other hand has $2N + 2$ states including circulating current, output current, and capacitor voltage for each SM. The corresponding dynamic equations are given below:

$$\begin{cases} \dfrac{di_o}{dt} = \dfrac{1}{2L_o + L}[(U_{N+1}V_{N+1} + U_{N+2}V_{N+2} \\ + \ldots + U_{2N}V_{2N}) - (U_1V_1 + U_2V_2 + \ldots + U_NV_N) - 2Ri_o] \\ \dfrac{di_c}{dt} = \dfrac{1}{2L}[V_{dc} - (U_{N+1}V_{N+1} + U_{N+2}V_{N+2} + \ldots + U_{2N} \\ V_{2N}) - (U_1V_1 + U_2V_2 + \ldots + U_NV_N)] \end{cases} \tag{6}$$

$$\begin{cases} \dfrac{dV_1}{dt} = \dfrac{U_1}{C} i_u \\ \vdots \\ \dfrac{dV_N}{dt} = \dfrac{U_N}{C} i_u \\ \dfrac{dV_{N+1}}{dt} = \dfrac{U_{N+1}}{C} i_l \\ \vdots \\ \dfrac{dV_{2N}}{dt} = \dfrac{U_{2N}}{C} i_l \end{cases} \tag{7}$$

where V_i is the voltage across capacitor of the i^{th} SM and U_i is the corresponding switching state, $i = 1, 2, \ldots, 2N$, and N is the number of SM's in each arm. The conventional indirect FCS-MPC utilizes the mathematical model defined in (1), whereas the direct FCS-MPC is implemented by using the model given by (6) and (7).

III. THE PROPOSED SINDY MODEL

Sparse identification of nonlinear dynamical systems (SINDy) uses noisy measurement data to determine the dynamics of a system [31]. Since the algorithm uses sparse regression, it generates the governing dynamic equations with the fewest terms possible. In this research, a generalized form of SINDy [32] is proposed to determine a reduced order dynamic system of MMCs in which input terms are also included in the dynamics.

Consider a nonlinear dynamical system given below:

$$\frac{d}{dt}x(t) = f(x(t), u(t)) \tag{8}$$

where $x \in \mathbb{R}^n$ is the state vector, $u \in \mathbb{R}^p$ is the input vector, and $f(x, u)$ are the nonlinear functions governing the system dynamics. For implementation, the state x and input u are sampled at different time instants $t_1, t_2, \ldots, t_m$. The derivatives $\dot{x}$ are assumed to be measured or approximated numerically using the state data. The state and input data can be stacked in two matrices given below:

$$X = \begin{bmatrix} x_1(t_1) & x_2(t_1) & \ldots & x_n(t_1) \\ x_1(t_2) & x_2(t_2) & \ldots & x_n(t_2) \\ \vdots & \vdots & \ddots & \vdots \\ x_1(t_m) & x_2(t_m) & \ldots & x_n(t_m) \end{bmatrix} \tag{9}$$

$$U = \begin{bmatrix} u_1(t_1) & u_2(t_1) & \ldots & u_p(t_1) \\ u_1(t_2) & u_2(t_2) & \ldots & u_p(t_2) \\ \vdots & \vdots & \ddots & \vdots \\ u_1(t_m) & u_2(t_m) & \ldots & u_p(t_m) \end{bmatrix} \tag{10}$$

A library of candidate functions $\Theta(X, U)$ can be constructed using the obtained data. A few examples of the candidate functions of X and U are constant, polynomial, trigonometric, and exponential terms or a combination of these terms:

$$\Theta(X, U) = [1^T \; X^T \; (X \circledast X)^T \; (X \circledast U)^T \; (U \circledast U)^T \ldots \times sin(X)^T \; sin(U)^T \; sin(X \circledast U)^T \ldots] \tag{11}$$

where $\circledast$ represents all the product combinations of the X and U vectors. Initially, a simple library of functions (polynomials) is chosen, and the complexity is increased by adding more terms like trigonometric functions. After selecting a specific library of functions, a sparse regression problem is set up to evaluate the sparse vectors of coefficients Ξ which determines the active nonlinearities. The system represented by (8) can be written in the following form:

$$\dot{X} = \Xi \Theta^T(X, U) \tag{12}$$

The time derivative $\dot{X}$ is computed numerically, if it can not be measured. The entries in each column of Ξ determines the active terms for each state dynamic equation. The solution for Ξ involves minimizing the following cost function:

$$\xi_i = argmin \frac{1}{2} ||\dot{X}_i - \hat{\xi}_i \Theta^T(X, U)||_2^2 + \lambda ||\hat{\xi}_i||_1 \tag{13}$$

where $\dot{X}_i$ and ξ_i are the i^{th} row of vectors $\dot{X}$ and Ξ, respectively. The 1-norm term $|.|_1$ introduces sparsity which can be controlled by adjusting the hyperparameter λ. The optimization problem defined in (13) can be solved using the LASSO [33] or the sequential thresholding least squares (STLSQ) [31] procedure.

A. PROPOSED SINDy MODEL FOR FCS-MPC IMPLEMENTATION ON MMCs

In the proposed method, a dynamical model of MMC using SINDy is developed at first:

Algorithm 1 Pseudo Code for the SINDy-Based Model Identification

1: Data collection to obtain i_c, i_o, v_u, v_l, n_u, and n_l signals to form the initial dataset X and U
$$X = [i_c \; i_o \; v_u \; v_l], \; U = [\, n_u \; n_l]$$
2: Compute numerical derivative of X to get $\dot{X}$
3: Choose appropriate candidate function $\Theta(X, U)$ and perform hyper-parameter λ settings based on greedy search.
4: Solve sparse regression problem using STLSQ algorithm
5: Get the final trained model in the form of
$$\dot{X} = f(x, u)$$

Utilizing the flexibility of choosing the candidate functions, input terms n_u and n_l are included in the dynamics of output and circulating currents. As output and circulating currents are the controlling parameters, the inclusion of input terms can greatly simplify the control design. It will also reduce the computational complexity of FCS-MPC as the voltage equations are not required to be solved during each step of FCS-MPC as is the case with the commonly used mathematical models, as shown in (1), (6)-(7). The obtained SINDy model is given below:

$$\begin{cases} \dfrac{di_c}{dt} = f_1(\Theta_1 = [X^T \; U^T]) \\ \dfrac{di_o}{dt} = f_2(\Theta_2 = [X^T \; U^T \; sin(X \circledast U)^T]). \end{cases} \tag{14}$$

Furthermore, by choosing different candidate functions, we can attain different models having different accuracies. For the current research, the circulating current dynamics only contain first-order polynomial terms, whereas the output current dynamics have first-order polynomial terms along with sinusoidal terms. It is possible to obtain a simpler or a more complicated model, depending on the requirements and the available data.

Remark 1: The SINDy model allows great flexibility in terms of the required complexity by selecting a specific library of candidate functions. Also, based on the nature and diversity of the training data, the model can help provide robustness against parameter uncertainties. Furthermore, the SINDy can generate accurate interpretable models under limited-data training, thereby reducing the training time as compared to NN and deep reinforced learning based models.

B. DATA ACQUISITION AND MODEL TRAINING

The model training involves two steps (1) Acquiring data, and (2) Training the model using the 'pysindy' library [34] developed in Python. These two steps are described below:

1) Data acquisition step: The training data is collected under different operating conditions at a selected sampling rate. For example, we need to collect samples of i_c, i_o, v_u, v_l, n_u, and n_l at each time step. The acquired data is then saved and transported to Python for model training.

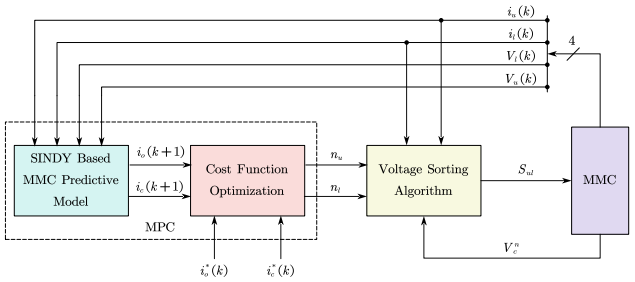

FIGURE 2. SINDy based FCS-MPC for MMCs.

2) Model training step: In this step, data acquired in the previous step is used to form the X and U matrices given by (9) and (10). The derivative matrix $\dot{X}$ is computed numerically using the finite difference method. The library of candidate functions is defined and the hyperparameter λ is selected. The model is trained for different variations of candidate functions and the hyperparameter by using the greedy search algorithm. Finally, the model is tested using the test samples.

After acquiring sufficient knowledge of the system behavior and setting the right parameters for the choice of library of candidate functions and the hyperparameter, the SINDy algorithm was able to generate the required model in less than 60s. The model training was performed using a computer equipped with 8 gigabyte RAM and an Intel core i5 2.40 GHz processor.

IV. FCS-MPC FORMULATION AND COST FUNCTION

The block diagram of the proposed MPC is shown in Fig. 2. In the presented indirect FCS-MPC scheme, control of output and circulating currents is performed, and inserted modules for the upper arm n_u and lower arm n_l are generated as output of the predictive control. The capacitor voltage balancing is performed outside the MPC, and a separate voltage balancing scheme is implemented to further reduce the computational load on the proposed FCS-MPC algorithm. In this section, we present a computationally efficient FCS-MPC control with improved THD and switching frequency using the obtained SINDy model. As the proposed scheme eliminates the need to use the voltage dynamics of upper and lower arms as shown in Eq. (1) and the SM capacitor voltage dynamics as seen in Eq. (6)-(7), the control becomes more efficient and the complexity is reduced. Additionally, since the model is data-driven, it can also capture the unmodelled dynamics. This will be observed in the model verification in which the circulating current response generated by SINDy outperforms the equivalent mathematical model response. Furthermore, in the existing work that implemented the indirect FCS-MPC on MMCs, it is assumed that the capacitors are perfectly balanced. This can cause prediction errors due to the presence of capacitor voltage ripples which can degrade the performance of the implemented control. Whereas in the proposed SINDy based FCS-MPC, since the model of the MMC is data-driven, the capacitor voltage ripples are indirectly captured in the system dynamics and the predicted states. Since the FCS-MPC relies on the accuracy of the system model, using the data-driven model reflecting capacitor voltage ripples can improve the tracking performance.

Remark 2: The reduction in computational complexity due to the proposed SINDy based FCS-MPC is validated in comparison to the conventional indirect FCS-MPC in a simulation setting with 10 SMs in each arm, and the results are included in Section V. It is observed that the SINDy based FCS-MPC is able to reduce the computation time by approximately 50%.

A. COST FUNCTION MINIMIZATION

The FCS-MPC optimization problem is formulated as:

$$\begin{aligned} min \quad & J(x(k+1), U(k)) \\ s.t. \quad & x_{k+1} = f(x(k), u(k)) \\ & U(k) = [u_1(k), u_2(k), \ldots, u_{(N+1)^2}(k)] \end{aligned} \tag{15}$$

where J is the cost function that needs to be minimized, f is the discrete-time system model, and U contains all the possible input switching combinations. In order to implement the FCS-MPC, the discrete-time model of MMC is required. The forward Euler approximation is used to discretize the SINDy model represented by (14). The obtained discrete-time model is given below:

$$i_c(k+1) = i_c(k) + T_s f_1(\Theta_1(k)) \tag{16}$$

$$i_o(k+1) = i_o(k) + T_s f_2(\Theta_2(k)) \tag{17}$$

where T_s is the sampling period, $k+1$ terms represent the predicted values, and k is the current sampling instant. Two different cost functions are used for this research and are given below:

$$J_1 = w_c(i_c^* - i_c(k+1))^2 + w_o(i_o^* - i_o(k+1))^2 \tag{18}$$

$$J_2 = w_c(i_c^* - i_c(k+1))^2 + w_o(i_o^* - i_o(k+1))^2 + w_u n_u + w_l n_l \tag{19}$$

where i_c^* is the circulating current reference, i_o^* is the output current reference, i_c is the predicted circulating current, i_o is the predicted output current, w_c, w_o, w_u, and w_l are the weights associated with the circulating current, output current, upper arm control input, and lower arm control input, respectively. As an indirect FCS-MPC using the SINDy model is implemented, the capacitor voltage terms are not included in the cost function in order to minimize the computational complexity and to ensure the solution remains viable.

The revised cost function defined in (19) provides a better response by reducing the THD and alleviating the effects of the high switching frequency problem caused by FCS-MPC. It tries to reduce the number of active switches, thereby increasing efficiency and reducing the chances of switch faults. However, it can slightly increase the tracking error as compared to the cost function represented by (18) due to the

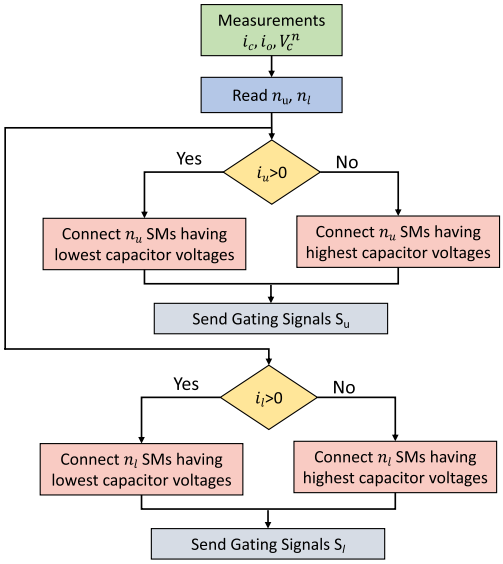

FIGURE 3. Capacitor voltage balancing flowchart.

inclusion of additional terms in the cost function that may compromise the minimization of tracking error terms.

Remark 3: The FCS-MPC control involves considering all the possible switching combinations for n_l and n_u to evaluate a cost function. The switching configuration in terms of the number of inserted SM for the upper and lower arms is selected which minimizes the defined cost function. Since the proposed MPC does not involve computing the dynamic equations of the SM capacitor voltages as in the case of (7) or the sum of capacitor voltages in the upper and lower arms defined in (1) to predict i_c and i_o, the computation burden is reduced. Furthermore, the inclusion of the weighting factor for n_u and n_l in the cost function reduces the switching frequency and the output THD without affecting the capacitor voltage balancing.

B. CAPACITOR VOLTAGE BALANCING

The voltage sorting algorithm given in [35] is adopted to perform the capacitor voltage balancing of the MMC. The algorithm decides the SMs to be inserted or bypassed based on the direction of the arm currents and the FCS-MPC outputs, i.e., n_u and n_l. In case when $i_{u,l} > 0$, the algorithm inserts n_u and n_l capacitors having the lowest voltages in the upper and lower arms, respectively. Conversely, in the event when $i_{u,l} < 0$, n_u and n_l capacitors having the highest voltages are inserted in the upper and lower arms. At each sample time, switching signals for each SM in the upper arm S_u and the lower arm S_l are obtained and applied based on the arm currents direction, capacitor voltages, and the obtained FCS-MPC outputs. The flowchart of the voltage sorting algorithm is presented in Fig. 3.

V. SIMULATION RESULTS

The simulation results are presented to show the effectiveness and characteristics of the proposed SINDy-FCS-MPC method. The simulation for the proposed technique is carried out in MATLAB/Simulink, whereas the SINDy model is trained using the 'pysindy' library developed in Python. The simulation parameters can be found in Table 1. In this section, the proposed SINDy model has been validated and compared to the mathematical model. Furthermore, the steady-state and transient performance of the proposed SINDy based indirect FCS-MPC has been evaluated and compared with the conventional indirect FCS-MPC approach.

TABLE 1. Simulation Parameters.

Parameters	Values
Load Inductance L_o	30 mH
Arm Inductance L	5 mH
Load Resistance R_o	10Ω
Capacitance C	10 mF
Input Voltage V_{dc}	1500 V
Number of cells per arm	10

A. SINDy MODEL VALIDATION

The SINDy model described by Eq. (14) has been rigorously tested under several conditions. The observed circulating current i_c and output current i_o from the SINDy model of MMC are compared with the ones obtained using the mathematical model as shown in Eq. (1). Fig. 4 shows the corresponding comparison between the measured i_c and i_o with the states generated using SINDy and the mathematical model. It can be observed from the shown results that i_o produced by both the models are close to the measured values. However, the circulating current i_c generated by the SINDy model outperforms the mathematical model by a fair margin.

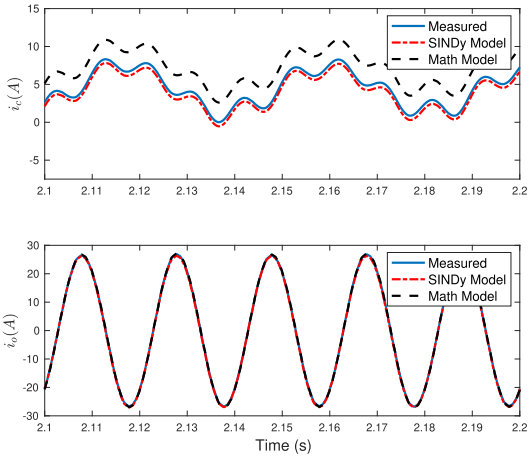

FIGURE 4. Model validation of the proposed SINDy model and its comparison with the mathematical model. From top to bottom (a). Circulating current, (b). Output current.

B. STEADY-STATE PERFORMANCE

The steady-state performance of the proposed SINDy FCS-MPC and the conventional indirect FCS-MPC is shown in Fig. 5 and 6, respectively. The reference for the output

current is set to an amplitude of 25A. It can be seen that the proposed approach and the conventional indirect FCS-MPC shows similar performance and are able to track the output current reference while keeping the circulating current sufficiently suppressed. However, a 10% improvement in the circulating current suppression is observed in the case of the proposed SINDy based FCS-MPC. Furthermore, in order to compare the computational complexity, Simulink profiler is used to compute the time that is required to evaluate the conventional indirect FCS-MPC and the proposed scheme under the same simulation settings. The submodule capacitor voltages are well balanced in both cases. Table 2 shows the comparison between the conventional indirect FCS-MPC and the proposed method based on the selected criteria.

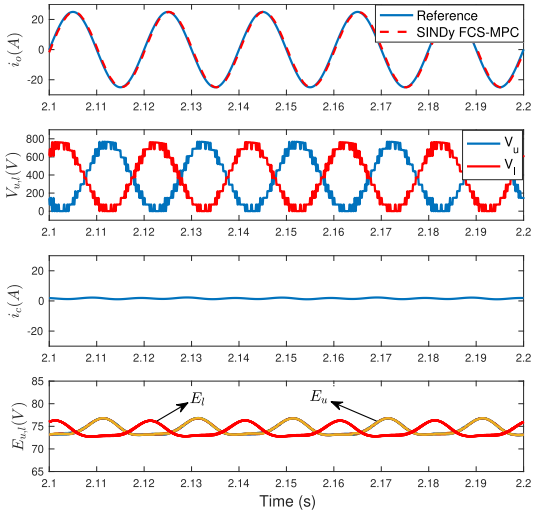

FIGURE 5. Simulation results of the steady-state response using the proposed SINDy based FCS-MPC. From top to bottom: (a). Output current, (b). Arm voltages, (c). Circulating current, and (d). Capacitor voltages.

C. TRANSIENT PERFORMANCE

The transient performance of the proposed algorithm is also investigated by changing the amplitude of the output current reference from 25A to 20A at 5s. As seen in Fig. 7, it can be noticed that the system remains stable during this step reference change and the output current is able to track the reference trajectory. The proposed technique is compared with the transient performance of the conventional indirect FCS-MPC as shown in Fig. 8. The voltages across the submodule capacitors are effectively balanced for both cases and the circulating current is also adequately suppressed. However, the SINDy based FCS-MPC generates better circulating current suppression while reducing the computational complexity. To observe the effect of adding input weight terms in the cost functions, Fig. 9 shows the switching signals produced from the proposed FCS-MPC. Since the added terms in the cost function J_2 do not allow abrupt changes to the switching signals, this results in lower switching frequency as compared to J_1 and provides a smoother response.

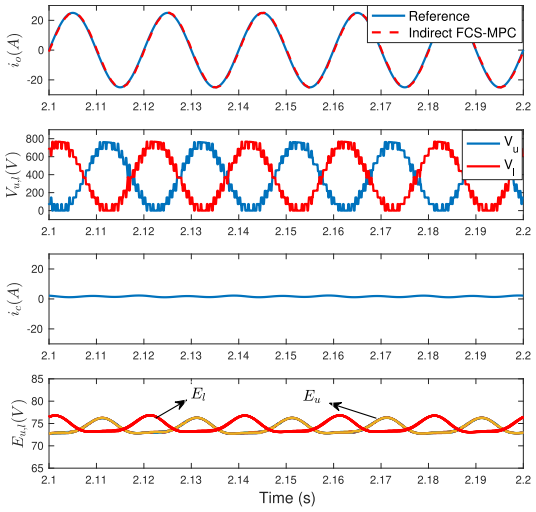

FIGURE 6. Simulation results of the steady-state response using the conventional indirect FCS-MPC. From top to bottom: (a). Output current, (b). Arm voltages, (c). Circulating current, and (d). Capacitor voltages.

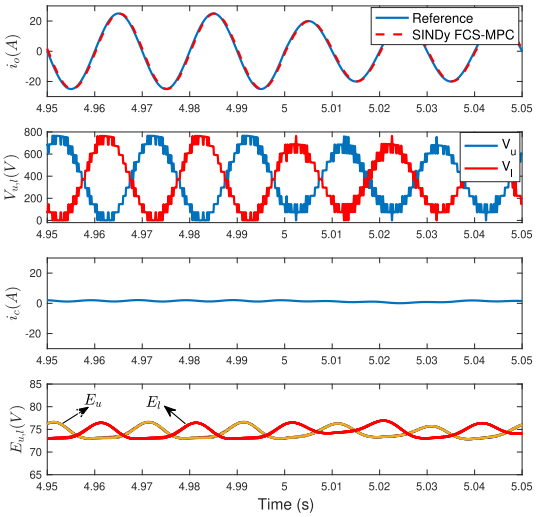

FIGURE 7. Simulation results of the transient response using the proposed SINDy based FCS-MPC. From top to bottom: (a). Output current, (b). Arm voltages, (c). Circulating current, and (d). Capacitor voltages.

TABLE 2. Comparison between conventional indirect FCS-MPC and SINDy FCS-MPC.

Criteria	Method	
	Conventional Indirect FCS-MPC	Proposed
Output current THD	0.6%	0.6%
Output current tracking	Excellent	Excellent
Circulating current (RMS)	0.63A	0.56A
Computation time	0.26s	0.13s

VI. EXPERIMENTAL RESULTS

The effectiveness of the proposed MPC approach is further validated on a 16-submodule singe-phase laboratory prototype. The digital controller is based on B-Box which is

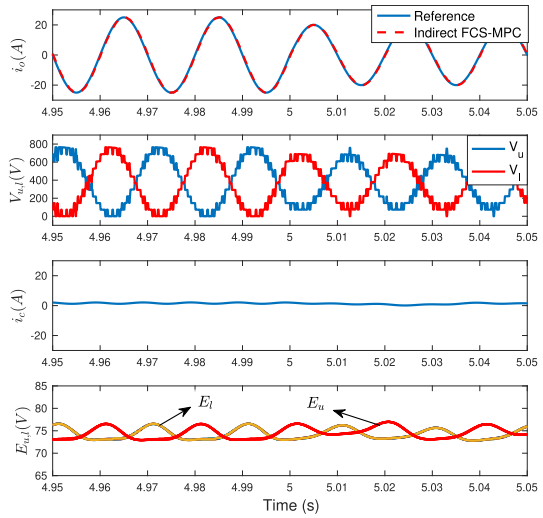

FIGURE 8. Simulation results of the transient response using the conventional indirect FCS-MPC. From top to bottom: (a). Output current, (b). Arm voltages, (c). Circulating current, and (d). Capacitor voltages.

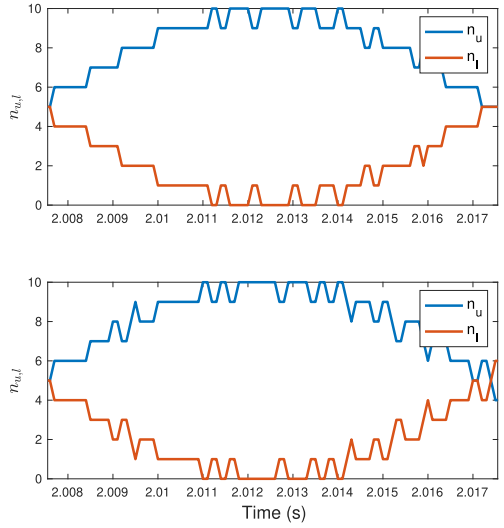

FIGURE 9. Switching signals for the two cost functions. From top to bottom: (a). With input weights, (b). Without input weights.

a real-time DSP+FPGA rapid prototyping controller. The experimental MMC test bench used for this research is shown in Fig. 10 and the system parameters are given in Table 3. The results depicted in Fig. 11 demonstrate that the SINDy model is more effective in approximating the actual measured states as compared to the mathematical model given by Eq. (1). The accuracy of the mathematical model is reduced by losses in the physical system, whereas the SINDy model is able to produce precise approximations.

The proposed algorithm is first tested under steady-state in which the output current reference is set to an amplitude of 12A. As seen in Fig. 12 the implemented control scheme performs well in tracking the reference trajectory and provides good circulating current suppression and the voltages across submodule capacitors are well balanced. Experimental

TABLE 3. Experimental Parameters.

Parameters	Values
Load Inductance L_o	10 mH
Arm Inductance L	5 mH
Load Resistance R_o	10.7Ω
Capacitance C	5000 μF
Input Voltage V_{dc}	320 V
Number of cells per arm	8

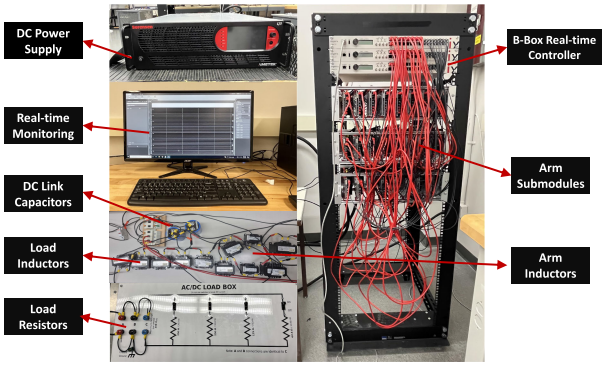

FIGURE 10. Experimental setup.

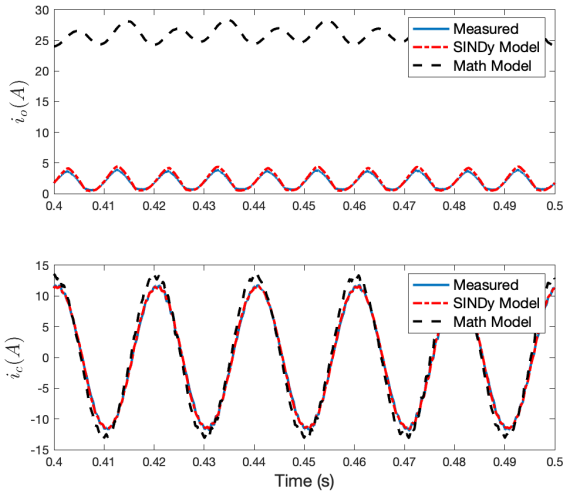

FIGURE 11. Model validation of the proposed SINDy model and its comparison with the mathematical model. From top to bottom: (a). Circulating current, (b). Output current.

TABLE 4. Comparison between conventional indirect FCS-MPC and SINDy FCS-MPC.

Criteria	Method	
	Conventional Indirect FCS-MPC	Proposed
Output current THD	2.1%	1.2%
Output current tracking	Excellent	Excellent
Circulating current (RMS)	2.05A	1.7A

results were also obtained for the conventional indirect FCS-MPC to compare the performances which is shown in Table 4. It was observed that the conventional indirect FCS-MPC

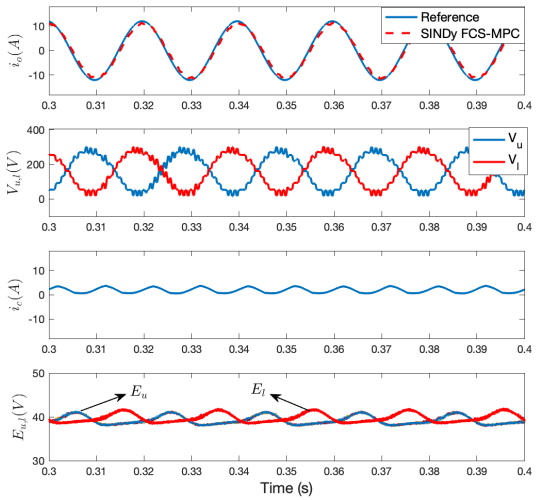

FIGURE 12. Experimental results of the steady-state response using the proposed SINDy based FCS-MPC. From top to bottom: (a). Output current, (b). Arm voltages, (c). Circulating current, and (d). Capacitor voltages.

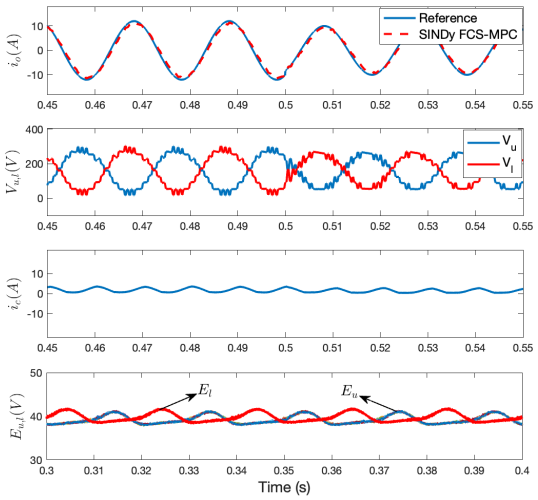

FIGURE 13. Experimental results of the transient response using the proposed SINDy based FCS-MPC. From top to bottom: (a). Output current, (b). Arm voltages, (c). Circulating current, and (d). Capacitor voltages.

yields a higher output current THD compared to the proposed FCS-MPC. Additionally, an improvement of 16% in the circulating current suppression was observed for the SINDy-FCS-MPC when compared with the conventional indirect FCS-MPC.

To verify the dynamic response of the proposed method, the output reference amplitude is changed from 12A to 10A at 0.5s. The generated results are shown in Fig. 13 for the proposed SINDy based FCS-MPC. It can be observed from these results that the system remains stable during the step reference change and the system is able to track the output current trajectory effectively. The capacitor voltages also remain balanced throughout the operation.

Finally, the effect of adding input weight terms in the cost function is evaluated by observing the switching

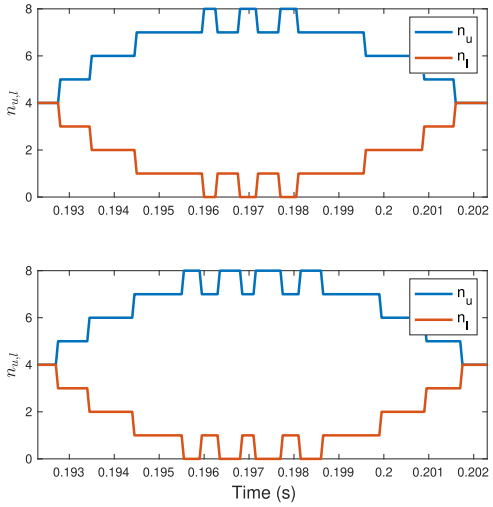

FIGURE 14. Switching signals for the two cost functions. From top to bottom: (a). With input weights, (b). Without input weights.

combinations generated by the FCS-MPC using the two cost functions J_1 and J_2 defined in (18)-(19). It is shown in Fig. 14 that the FCS-MPC which uses J_2 as the cost function results in lower switching frequency, therefore ensuring better system efficiency and increased reliability.

VII. CONCLUSION AND FUTURE WORK

This paper presents the design and implementation of an indirect FCS-MPC for MMCs by developing a reduced state data-driven model using SINDy. In the reduced model, only the circulating current and load current dynamics are used for the implementation of the FCS-MPC. This is accomplished by adding the dependencies of the input terms, i.e., n_u and n_l in the dynamics of i_c and i_o. Doing so removes the need to use the corresponding SM voltages or the sum of capacitor voltages dynamics. To further reduce the computational complexity and to make the control simple, the capacitor voltage balancing is decoupled from the actual control and performed in a separate block.

In addition to reducing the computational complexity, the effect of the abrupt switching caused by MPC is also reduced by using an updated cost function having weighting factors with the inputs alongside the control terms. Using this cost function allows a decrease in the THD of the load current and reduces the unnecessary switching caused by the FCS-MPC, hence increasing reliability and efficiency.

In the future, the proposed scheme can open a new direction for using interpretable data-driven models for implementing MPC control in power systems. The performance of FCS-MPC can further be improved by using optimally tuned weighting factors. Similarly, designing controls that are robust against parameter uncertainties is an active research in MMCs. This control problem can be solved by using a SINDy based model and incorporating the relevant parameter uncertainties conditions in the training data. It can also have many applications in fault diagnosis of MMCs as the SINDy

generated model can provide better approximations of the system states that can help develop robust fault diagnosis methods.

REFERENCES

[1] G. P. Adam, I. Abdelsalam, J. E. Fletcher, G. M. Burt, D. Holliday, and S. J. Finney, "New efficient submodule for a modular multilevel converter in multiterminal HVDC networks," *IEEE Trans. Power Electron.*, vol. 32, no. 6, pp. 4258–4278, Jun. 2017.

[2] S. Du, B. Wu, N. R. Zargari, and Z. Cheng, "A flying-capacitor modular multilevel converter for medium-voltage motor drive," *IEEE Trans. Power Electron.*, vol. 32, no. 3, pp. 2081–2089, Mar. 2017.

[3] N. Li, F. Gao, T. Hao, Z. Ma, and C. Zhang, "SOH balancing control method for the MMC battery energy storage system," *IEEE Trans. Ind. Electron.*, vol. 65, no. 8, pp. 6581–6591, Aug. 2017.

[4] B. Fan, Y. Li, K. Wang, Z. Zheng, and L. Xu, "Hierarchical system design and control of an MMC-based power-electronic transformer," *IEEE Trans. Ind. Informat.*, vol. 13, no. 1, pp. 238–247, Feb. 2017.

[5] Q. Yang, M. Saeedifard, and M. A. Perez, "Sliding mode control of the modular multilevel converter," *IEEE Trans. Ind. Electron.*, vol. 66, no. 2, pp. 887–897, Feb. 2019.

[6] F. Deng and Z. Chen, "Voltage-balancing method for modular multilevel converters under phase-shifted carrier-based pulsewidth modulation," *IEEE Trans. Ind. Electron.*, vol. 62, no. 7, pp. 4158–4169, Jul. 2015.

[7] B. Bahrani, S. Debnath, and M. Saeedifard, "Circulating current suppression of the modular multilevel converter in a double-frequency rotating reference frame," *IEEE Trans. Power Electron.*, vol. 31, no. 1, pp. 783–792, Jan. 2016.

[8] X. Li, Q. Song, W. Liu, S. Xu, Z. Zhu, and X. Li, "Performance analysis and optimization of circulating current control for modular multilevel converter," *IEEE Trans. Ind. Electron.*, vol. 63, no. 2, pp. 716–727, Feb. 2016.

[9] J. Rodriguez, M. P. Kazmierkowski, J. R. Espinoza, P. Zanchetta, H. Abu-Rub, H. A. Young, and C. A. Rojas, "State of the art of finite control set model predictive control in power electronics," *IEEE Trans. Ind. Informat.*, vol. 9, no. 2, pp. 1003–1016, May 2013.

[10] S. Vazquez, J. Rodriguez, M. Rivera, L. G. Franquelo, and M. Norambuena, "Model predictive control for power converters and drives: Advances and trends," *IEEE Trans. Ind. Electron.*, vol. 64, no. 2, pp. 935–947, Feb. 2017.

[11] X. Liu, L. Qiu, W. Wu, J. Ma, Y. Fang, Z. Peng, and D. Wang, "Event-triggered neural-predictor-based FCS-MPC for MMC," *IEEE Trans. Ind. Electron.*, vol. 69, no. 6, pp. 6433–6440, Jun. 2022.

[12] M. Majstorovic, M. Rivera, L. Ristic, and P. Wheeler, "Comparative study of classical and MPC control for single-phase MMC based on V-HIL simulations," *Energies*, vol. 14, no. 11, p. 3230, May 2021.

[13] J. Bocker, B. Freudenberg, A. The, and S. Dieckerhoff, "Experimental comparison of model predictive control and cascaded control of the modular multilevel converter," *IEEE Trans. Power Electron.*, vol. 30, no. 1, pp. 422–430, Jan. 2015.

[14] T. Dragičević, "Model predictive control of power converters for robust and fast operation of AC microgrids," *IEEE Trans. Power Electron.*, vol. 33, no. 7, pp. 6304–6317, Jul. 2017.

[15] K. Wang, Z. Zheng, L. Xu, and Y. Li, "Neutral-point voltage balancing method for five-level NPC inverters based on carrier-overlapped PWM," *IEEE Trans. Power Electron.*, vol. 36, no. 2, pp. 1428–1440, Feb. 2021.

[16] K. Wang, Z. Zheng, L. Xu, and Y. Li, "A generalized carrier-overlapped PWM method for neutral-point-clamped multilevel converters," *IEEE Trans. Power Electron.*, vol. 35, no. 9, pp. 9095–9106, Sep. 2020.

[17] J.-W. Moon, J.-S. Gwon, J.-W. Park, D.-W. Kang, and J.-M. Kim, "Model predictive control with a reduced number of considered states in a modular multilevel converter for HVDC system," *IEEE Trans. Power Del.*, vol. 30, no. 2, pp. 608–617, Apr. 2015.

[18] J. Qin and M. Saeedifard, "Predictive control of a modular multilevel converter for a back-to-back HVDC system," *IEEE Trans. Power Del.*, vol. 27, no. 3, pp. 1538–1547, Jul. 2012.

[19] M. Vatani, B. Bahrani, M. Saeedifard, and M. Hovd, "Indirect finite control set model predictive control of modular multilevel converters," *IEEE Trans. Smart Grid*, vol. 6, no. 3, pp. 1520–1529, May 2015.

[20] P. Liu, Y. Wang, W. Cong, and W. Lei, "Grouping-sorting-optimized model predictive control for modular multilevel converter with reduced computational load," *IEEE Trans. Power Electron.*, vol. 31, no. 3, pp. 1896–1907, Mar. 2016.

[21] A. Rashwan, M. A. Sayed, Y. A. Mobarak, G. Shabib, and T. Senjyu, "Predictive controller based on switching state grouping for a modular multilevel converter with reduced computational time," *IEEE Trans. Power Del.*, vol. 32, no. 5, pp. 2189–2198, Oct. 2017.

[22] B. Gutierrez and S.-S. Kwak, "Modular multilevel converters (MMCs) controlled by model predictive control with reduced calculation burden," *IEEE Trans. Power Electron.*, vol. 33, no. 11, pp. 9176–9187, Nov. 2018.

[23] S. Wang, T. Dragicevic, G. F. Gontijo, S. K. Chaudhary, and R. Teodorescu, "Machine learning emulation of model predictive control for modular multilevel converters," *IEEE Trans. Ind. Electron.*, vol. 68, no. 11, pp. 11628–11634, Nov. 2021.

[24] M. Vasiladiotis, A. Christe, and T. Geyer, "Model predictive pulse pattern control for modular multilevel converters," *IEEE Trans. Ind. Electron.*, vol. 66, no. 3, pp. 2423–2431, Mar. 2019.

[25] V. Spudic and T. Geyer, "Model predictive control based on optimized pulse patterns for modular multilevel converter STATCOM," *IEEE Trans. Ind. Appl.*, vol. 55, no. 6, pp. 6137–6149, Nov. 2019.

[26] H. Akaike, "Fitting autoregressive models for prediction," *Ann. Inst. Stat. Math.*, vol. 21, no. 1, pp. 243–247, Dec. 1969.

[27] S. A. Billings, *Nonlinear System Identification: Narmax Methods in the Time, Frequency, and Spatio-Temporal Domains*. NJ, USA: Wiley, 2013.

[28] H. Peng, J. Wu, G. Inoussa, Q. Deng, and K. Nakano, "Nonlinear system modeling and predictive control using the RBF nets-based quasi-linear ARX model," *Control Eng. Pract.*, vol. 17, no. 1, pp. 59–66, 2009. [Online]. Available: https://www.sciencedirect.com/science/article/pii/S0967066108000993

[29] T. Zhang, G. Kahn, S. Levine, and P. Abbeel, "Learning deep control policies for autonomous aerial vehicles with MPC-guided policy search," 2015, *arXiv:1509.06791*.

[30] R. T. Q. Chen, Y. Rubanova, J. Bettencourt, and D. Duvenaud, "Neural ordinary differential equations," 2018, *arXiv:1806.07366*.

[31] S. L. Brunton, J. L. Proctor, and J. N. Kutz, "Discovering governing equations from data by sparse identification of nonlinear dynamical systems," *Proc. Nat. Acad. Sci. USA*, vol. 113, no. 15, pp. 3932–3937, 2015, doi: 10.1073/pnas.1517384113.

[32] E. Kaiser, J. N. Kutz, and S. L. Brunton, "Sparse identification of nonlinear dynamics for model predictive control in the low-data limit," *Proc. Roy. Soc. A, Math., Phys. Eng. Sci.*, vol. 474, no. 2219, Nov. 2018, Art. no. 20180335, doi: 10.1098/rspa.2018.0335.

[33] R. Chartrand, "Numerical differentiation of noisy, nonsmooth data," *ISRN Appl. Math.*, vol. 2011, pp. 1–11, May 2011.

[34] A. Kaptanoglu, B. de Silva, U. Fasel, K. Kaheman, A. Goldschmidt, J. Callaham, C. Delahunt, Z. Nicolaou, K. Champion, J.-C. Loiseau, J. Kutz, and S. Brunton, "PySINDy: A comprehensive Python package for robust sparse system identification," *J. Open Source Softw.*, vol. 7, no. 69, p. 3994, Jan. 2022, doi: 10.21105/joss.03994.

[35] Z. Gong, P. Dai, X. Yuan, X. Wu, and G. Guo, "Design and experimental evaluation of fast model predictive control for modular multilevel converters," *IEEE Trans. Ind. Electron.*, vol. 63, no. 6, pp. 3845–3856, Jun. 2016.

MUNEEB MASOOD RAJA received the B.E. degree in mechatronics engineering from the National University of Sciences and Technology (NUST), Pakistan, and the M.S. degree in electrical engineering from Wright State University (WSU), USA. He is currently pursuing the Ph.D. degree in electrical and computer engineering with the University of Alberta, Canada.

From 2015 to 2017, he was a Research Assistant with WSU. He was a Lecturer with NUST, from 2017 to 2020. His current research interests include data-driven control techniques, state estimation, fault diagnosis, and fault tolerant control of power converters.

HAORAN WANG received the B.Sc. degree in electrical engineering from the Shenyang University of Technology, Shenyang, China, in 2019. He is currently pursuing the Ph.D. degree with the Electrical and Computer Engineering Department, University of Alberta, Edmonton, Canada. His current research interests include modular multilevel converter, HVDC, fault diagnosis, and fault tolerant control.

MUHAMMAD HASEEB ARSHAD received the B.Sc. degree in electrical engineering from the University of the Punjab, Lahore, Pakistan, and the M.Sc. degree in electrical engineering from the King Fahd University of Petroleum and Minerals, Dhahran, Saudi Arabia. He is currently pursuing the Ph.D. degree in control engineering with the Electrical and Computer Engineering Department, University of Alberta, Edmonton, Canada.

His research interests include time series anomaly detection, fault detection for MMCs, machine learning-based digital twin models for power systems, optimal power flow for dc microgrids, variable speed drives for multiphase induction motor, adversarial learning for deep learning models targeted towards computer vision, digital filter designs, and the robust control of nonlinear systems.

GREGORY J. KISH (Senior Member, IEEE) received the B.E.Sc. degree in electrical engineering from the University of Western Ontario, Canada, and the M.A.Sc. and Ph.D. degrees in electrical engineering from the University of Toronto, Canada. He is currently an Associate Professor with the University of Alberta, Canada. His research interest includes the development and application of power electronic converter systems in electric grids.

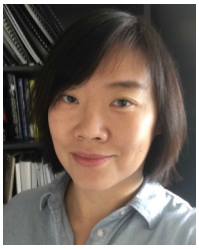

QING ZHAO (Member, IEEE) received the B.Sc. degree in control engineering from Northeastern University (NEU), China, and the Ph.D. degree in electrical engineering from the University of Western Ontario (now the Western University), Canada.

She was a Visiting Professor with the Control Engineering Department, University Libre de Bruxelles, Brussels, Belgium, from August to December 2008. She held an Alexander von Humboldt Research Fellowship and was a Visiting Professor with the University of Duisburg-Essen, Duisburg, Germany, from January to July 2009. She is currently a Professor with the Department of Electrical and Computer Engineering, University of Alberta, Canada. Her current research interests include fault diagnosis, fault tolerant control, robust control, optimal control and estimation, machine condition monitoring, and process and data analytics.